The Geographic Base

Journal Homepage: https://www.ngssnepal.org/journal

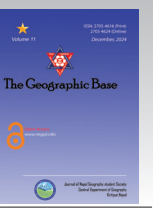

Land Surface Temperature and Its Correlation with Normalized Difference Spectral Indices

Shudarshan Hamal [1], Binita Shahi [2, *], Sudeep Thakuri [3], Prashamsa Shrestha [4]

[1]Central Department of Environmental Science, Institute of Science and Technology, Tribhuvan University, Kirtipur, 44613 Kathmandu, Nepal. **ORCID iD**: https://orcid.org/0009-0008-4828-5363

[2]College of Applied Science, Institute of Science and Technology, Tribhuvan University, Thapathali, 44600 Kathmandu, Nepal. **ORCID iD:** https://orcid.org/0009-0001-3098-8369

[3]Graduate School of Science and Technology, Mid-West University, 21700 Birendranagar, Nepal.

[4]Naaya Aayam Multi-Disciplinary Institute (NAMI), University of Northampton, Baneshwor, 44600 Kathmandu, Nepal. **ORCID iD:** https://orcid.org/0000-0002-5278-9985

*** Corresponding Author:** binitathakuri111@gmail.com

Article info

Keywords:
LST, Nepalgunj, NDBI, NDVI

Received: 5th April 2024

Accepted: 10th July 2024

DOI: https://doi.org/10.3126/tgb.v11i01.88629

Abstract

Land surface temperature and vegetation indices have been explored as indicators for various environmental variables. A number of research papers have normalized difference vegetation index as an approximation of density, and urban expansion depends on normalized difference build-up index of Nepalgunj urban area ranging from 2013 to 2022. Based on Landsat 8 satellite images, it investigates impacts on thermal conditions, vegetation and settlements and retains strong trends for environmental transformation. The result obtained revealed a very strong positive relationship between LST and NDBI (r^2 = 0.6042 to 0.7743), denoting a higher level of urban growth and hence an increased surface temperature. Similarly, there is a very strong negative relationship between LST and NDVI (r2 = -0.3165 to -0.5524), which shows that an increase in temperature

will have a damaging effect on health of vegetation. Moreover, an inversely proportional relationship between NDVI and NDBI has been found an explicit compromise between urban expansion and vegetative cover. These results are imperative for formulating and implementing the effects of UHI.

Introduction

Urbanization is a global phenomenon where land surfaces are massively altered and changed. Environmental dynamics along with it directly affects climate patterns (Chapagain, 2018; Hulley, 2012). Within fast-growing cities such as Nepalgunj, rapid expansion in the built-up area and land-use conversion of Natural landscapes into hard surfaces result in notible changes to local temperature and plant (Hamal et al. 2022; Tariq & Shu 2020).

Land surface temperature is central in environmental and climate research. It reflects the combined effect of various climatic and geophysical parameters such as soil moisture, vegetation, and air temperature. The thermal regime at the Earth's surface directly impacts on human comfort, energy needs, and microclimates within cities. Remote Sensing technology has enabled monitoring of LST and its relationship to other environmental factors such as-Vegetation and urban growth (Kalma et al., 2008). One of the most common vegetation indices is the Normalized Difference Vegetation Index (NDVI). This provides key information related to plant health and its response to temperature changes (Carlson et al., 1994). On the contrary, the Normalized Difference Built-up Index (NDBI) measures the urban density effectively and quantifies how much the built structures along with hard layers have spread in a region that eventually causes changes in the surface temperature (Zha et al., 2003).

While multispectral satellite imagery is one of the important sources of data for understanding urban dynamics. RS data Vegetation, water bodies, and urban growth can be monitored over time with precision and affordability (Ahmadi & Nusrath, 2010; Bhandari et al., 2012; Roy et al., 2017). The improvement of Satellite technology, particularly Landsats, have enabled observations to be made of the pattern of urban growth, plant health, and surface temperatures (Jat et al., 2008; Singha et al., 2022; Valor & Caselles, 1996). RS data helps the researchers in identifying the main environmental indicators, including NDVI and NDBI, which provide important information on the interaction between vegetation and urbanization.

LST is becoming more important in the evaluation of surface energy and water balances in urban areas. There is typically higher surface temperature in cities than in rural areas due to urban heat. Urban Heat Island (UHI) effect usually is a common phenomenon where lands trap heat due to human activities and high concentration of buildings, roads, and

other infrastructure (Cao et al., 2008; Kim, 1992; Wang &Akbari, 2017). In this context, this study discusses and examines how Nepalgunj, one of the fastest-growing sub-metropolitan cities is experiencing warming effects and impacts on vegetation, health, and urban planning.

Urbanization in Nepal has increased rapidly due to rural-to-urban migration and population demographics are different in various ways (Bhattarai & Conway, 2021). It has engendered disparate influences brought on by changes in population demographics. As urban populations increase, there are major land-use changes. Green spaces and natural soil give the way to concrete, asphalt, and other impervious surfaces (Kuang et al., 2016; Wigginton et al., 2016). These changes worsen UHI effects, making the local environments warmer compared to rural areas. Increased LST degrades vegetation density, disrupt natural growth patterns, and contribute to declines in biodiversity and the ecosystem services breakdown (Hamal et al., 2022; Kandel et al., 2022).

According to the current research, LST is generally directly proportional to urban areas. Normalized Difference Built-up Index (NDBI), with the interpretation that higher temperatures are associated with increased built-up density (Zha et al., 2003). In contrast, an opposite relationship between LST and NDVI is in close correspondence, which can be interpreted to mean that with increasing temperatures, vegetation health declines (Macarof & Statescu, 2017). These Connections mean everything to understand how local ecosystems are affected by urban growth and in shaping sustainable land-use plans. The study focuses on the changes in LST, NDVI, and NDBI in Nepalgunj, years ranging from 2013 to 2022. The aim is to assess how urbanization has impacted the variation in temperature. Changes in vegetation health and built-up area distribution will therefore be quite useful information for land-use planning and sustainable development.

Methods and Materials

Study area

Nepalgunj is a city located in the western Terai belt of Nepal in the Banke district, spanning from 28°8′1.12″N to 27°59′48.24″N latitude and 81°35′9.86″E to 81°42′11.91″E longitude as shown in Figure 1. The sub-metropolitan city is growing quickly. The city has grown remarkably over the last few decades due to increased migration, improved infrastructure, and economic opportunities, making it one of Nepal's most rapidly developing urban areas. According to the 2021 National Population Census, the city's 85.94 km² area is home to about 164,444 people, or an average of 1,913 people per km². The urban landscape has been drastically altered by this rapid development, which has changed the interaction between vegetation cover, surface temperature patterns, and growing built-up areas.

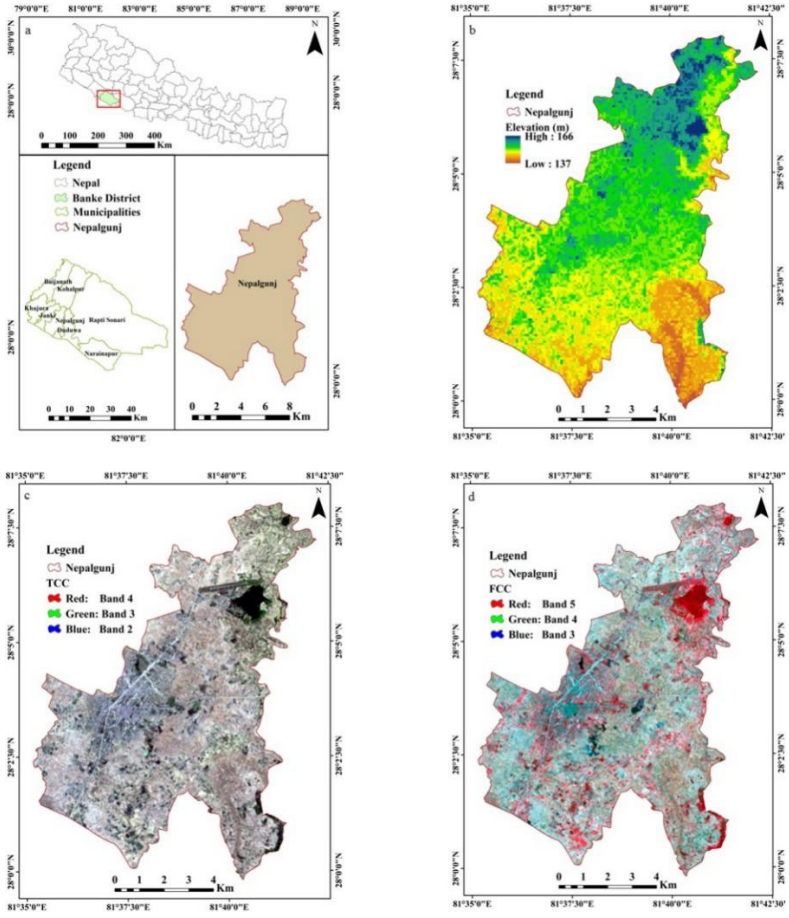

Figure 1. Location map of (a) Nepalgunj City of Banke District in Nepal, along with the (b) elevation, (c) TCC image, and (d) FCC image

Nepalgunj experiences a sub-tropical climate with hot summers during April–June, when temperatures go above 40 °C (Subedi1 et al., 2022; Weather Atlas, 2023). According to the DHM (2014), maximum temperature recorded historically was 45 °C while in 1995 and 2012 (DHM, 2014). The region is also vulnerable to heatwaves and seasonal flood, especially in the monsoon season with an average annual precipitation of approximately 1172 mm (Chhetri et al., 2020). These expanding cities are replacing natural landscape with artificial surfaces more and more rapidly such that the phenomenon of UHI is rapidly increasing. This study attempts to explore the interaction of these environmental drivers and investigate how rapid urbanization is affecting local climate in Nepalgunj.

Data acquisition

In this research, the authors used multitemporal Landsat 8 OLI/TIRS datasets from 2013 to 2022. Every scene provides a spatial resolution of 30 m for most spectral bands, making those scenes appropriate for vegetation cover, land use, and land surface thermal pattern change analysis. The dates in October and November were selected with the purpose of minimizing cloud interference, hence ensuring their high quality for further processing (Khan et al., 2022). Precisely, Table 1 describes the summary of the used Landsat imagery in this research, including acquisition dates, sensor configuration, path/row, and cloud coverage in percentage Table 1.

Table 1. Landsat imagery used for the study

Acquisition date	Satellite	Product scene identifier	Sensor	Band used	Path/Row	Resolution	Cloud cover
2013/11/16	Landsat 8	LC81430412013320LGN01	OLI-TIRS	4,5,6,10	143/041	30	0.07
2016/11/08	Landsat 8	LC81430412016313LGN01	OLI-TIRS	4,5,6,10	143/041	30	0.11
2019/10/16	Landsat 8	LC81430412019289LGN00	OLI-TIRS	4,5,6,10	143/041	30	0.74
2022/10/24	Landsat 8	LC81430412022297LGN00	OLI-TIRS	4,5,6,10	143/041	30	0.03

The datasets were obtained from the United States Geological Survey (USGS) Earth Explorer portal (https://earthexplorer.usgs.gov/). Landsat 8 offers 11 spectral bands; each tailored for specific surface features that range from vegetation to built-up surfaces and thermal emissions. The wavelength ranges and the spatial resolutions adopted in this study are provided in Table 2.

Table 2. Spectral characteristics of Landsat 8 bands

Bands	Wavelength (μm)	Resolution (m)
Band 1 - Ultra Blue (coastal/aerosol)	0.435 - 0.451	30
Band 2 - Blue	0.452 - 0.512	30
Band 3 - Green	0.533 - 0.590	30
Band 4 - Red	0.636 - 0.673	30
Band 5 - Near Infrared (NIR)	0.851 - 0.879	30
Band 6 - Shortwave Infrared 1 (SWIR1)	1.566 - 1.651	30
Band 7 - Shortwave Infrared 2 (SWIR2)	2.107 - 2.294	30
Band 8 - Panchromatic	0.503 - 0.676	15
Band 9 - Cirrus	1.363 - 1.384	30
Band 10 - Thermal Infrared 1 (TIRS1)	10.60 - 11.19	100 * (30)
Band 11 - Thermal Infrared 2 (TIRS2)	11.50 - 12.51	100 * (30)

Data pre-processing

Before analysis, several pre-processing operations were carried out to enhance geometric and radiometric quality:

Geometric correction was performed to align all images to the Universal Transverse Mercator (UTM) projection, Zone 44N, based on the WGS84 datum, using an image-to-image co-registration approach.

Radiometric calibration was conducted through the Semi-Automatic Classification Plugin in QGIS 3.28.13.

Additional geometric refinements were applied in ArcGIS 10.8 to ensure accurate spatial alignment.

The Banke District shapefile was used to subset the study area, restricting the analysis to the region of interest.

The overall processing workflow is presented in Figure 2.

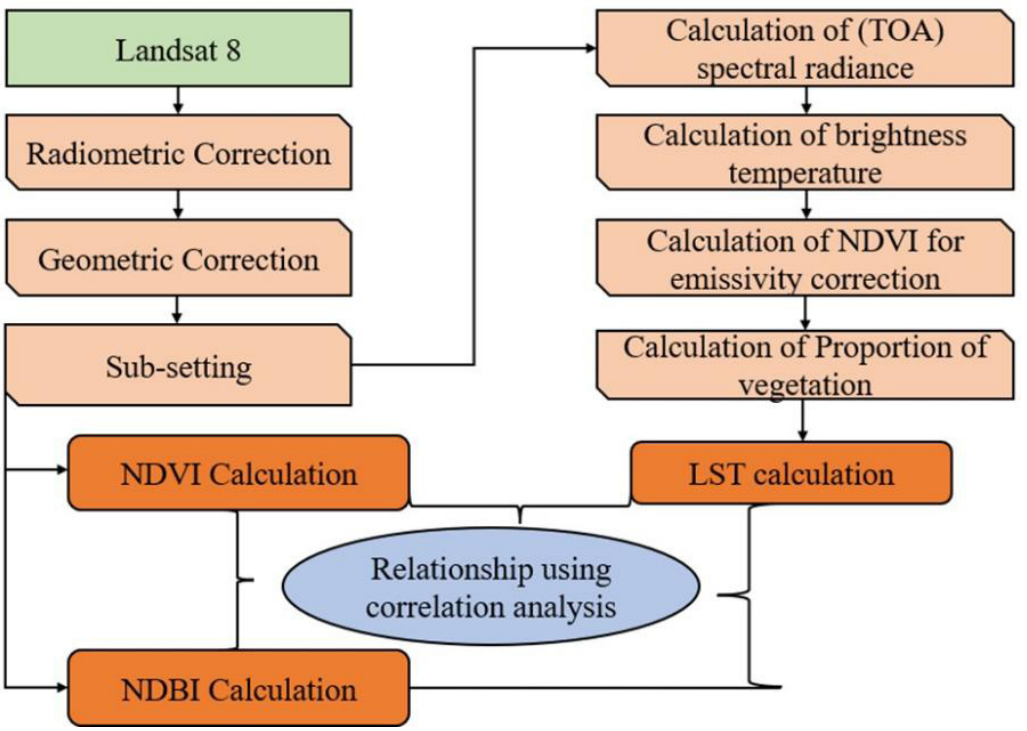

Figure 2. Methodology adopted for the study.

Computation of LST

(a) Conversion of digital number to top of atmosphere (TOA) radiance

The thermal band's digital numbers (DN) were transformed into spectral radiance (Lλ) using the following Equation 1 (Haylemariyam, 2018).

Equation 1

$$L\lambda = \left(\frac{LMAX\lambda - LMIN\lambda}{QCALMAX - QCALMIN}\right) \times (QCAL - QCALMIN) + LMIN\lambda \quad (1)$$

Where:

QCALMAX = 255 is the maximum quantized DN

QCALMIN = 1 is the minimum DN

LMAX and LMIN are radiance scaling factors obtained from the image metadata

(b) Conversion of radiance into brightness temperature

The derived radiance was converted to brightness temperature (T) in Kelvin using Equation 2

Equation 2

$$T = \frac{K_2}{ln\left(\frac{K_1}{L\lambda + 1}\right)} \quad (2)$$

Where K_2 and K_1 are sensor calibration constants. Finally, temperatures were converted from Kelvin to Celsius using Equation 3.

Equation 3

$$T(\circ C) = T(K) - 273 \quad (3)$$

(c) Calculation of NDVI for emissivity correction

The NDVI was used to estimate vegetation cover for emissivity correction (Huete & Liu, 1994; Leprieur et al., 2000; Putri et al., 2021) as in Equation 4.

Equation 4

$$NDVI = \frac{NIR - RED}{NIR + RED} \quad (4)$$

(d) Proportion of vegetation (PV)

From the maximum and minimum NDVI, the proportion of vegetation (PV) was computed using Equation 5.

Equation 5

$$PV = \left(\frac{NDVI - NDVImin}{NDVImax + NDVImin}\right)^2 \quad (5)$$

(e) Land surface emissivity (LSE)

LSE was determined using the following relationship as in Equation 6 (Jiménez-Muñoz et al., 2009).

Equation 6

$$\varepsilon = 0.004 \times Pv + 0.986 \quad (6)$$

(f) Land surface temperature (LST)

The LST was obtained from the brightness temperature and computed emissivity using *Equation 7*

$$T = BT\left[1 + \left\{\left(\frac{\lambda BT}{\rho}\right) ln\varepsilon\lambda\right\}\right] \quad (7)$$

Where:

BT = brightness temperature

λ = 10.895 μm = central wavelength

ελ = the computed emissivity

The categorization of LST, based on the analysis criteria, is presented in Table 3 as described by Sasky et al. (2017).

Table 3. Land surface temperature categorization

S.N.	LST class	Description
1	Very low	< 20°C
2	Low	20 °C - 25 °C
3	Medium	25 °C - 30 °C
4	High	30 °C - 35 °C
5	Very High	> 35 °C

Source: Sasky et al. (2017)

NDBI

The NDBI was calculated (Zha et al., 2003) using delineate urbanized areas Equation 8.

Equation 8

$$NDBI = \frac{SWIR - NIR}{SWIR + NIR} \quad (8)$$

Where:

SWIR = Shortwave Infrared reflectance (Band 6),

NIR = Near Infrared reflectance (Band 5).

Results and Discussion

Analysis of vegetation and built-up indices

It shows notable changes over time on the temporal variation of NDVI and NDBI representing changes from 2013 to 2022. land use and vegetation dynamics of Nepalgunj Figure 3. There is an inverse relation between NDVI and NDBI confirming that there is a loss or reduction of green cover and vegetation in the process of urbanization. While the mean NDBI value increased gradually from approximately -0.1387 in 2013 to approximately -0.0024 in 2022, this evidences gradual but continuing changes towards higher urbanization. On the contrary, the mean NDVI value varied from almost from 0.1333 in 2013 to 0.1974 in 2022, there were slight increases in vegetation density since there is a lot of variability within the study period. These patterns and trends are similar to as those recorded for the surrounding areas in Nepal, where urbanization has been connected to increasing values of NDBI and declining vegetation cover (Bhomi 2024). Besides that, the growing built areas may reduce the water retention capacity of the landscapes, thus affecting other hydrological indicators, such as Normalized Difference Water Index (NDWI) as proposed in work by (Shah et al., 2022). This can alter the hydrological balance by affecting surface water runoff and evaporation rates, and it has also got considerable connotation for proper land use and water management. Maximum NDVI indicated an increasing trend in the research period, but was a bit lower. Lost in 2016 due to human activities involving land development. Minimum NDVI

values varied: the same had remained constant for the years 2013 and 2016, while its sharp fall was registered in 2019, with a significant increase in 2022. This could be natural seasonality or human-induced changes, like deforestation, urbanization, or land use cover.

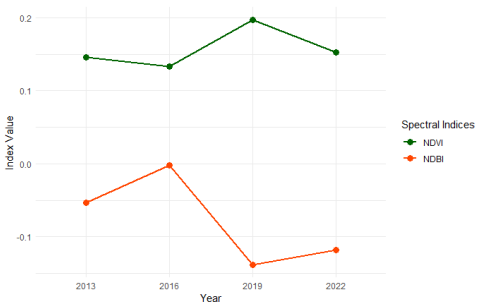

Figure 3. Average NDVI and NDBI change over 2013 -2022

Usually, high values of NDVI are indicative of high biomass areas with dense and healthy vegetation, whereas low values are typical for barren areas and areas dominated by non-vegetative land use. Higher values of NDVI also indicate that vegetation stays healthy for more days, mostly due to the availability of adequate soil moisture. A decline in NDVI in the year 2016 might relate to a decrease in soil water content, which has also been reported in some earlier studies.

The NDBI pattern shows that, in 2016, urbanization increased and produced the highest values that year, reduced in 2019, and partially recovered in 2022 (Figure 3). That reflects the straightforward relationship between increasing urban growth with the growth of hard surfaces at the expense of vegetation. Similar results have also been reported in previous studies (Karanam & Neela, 2017; Khan et al., 2022; Macarof & Statescu, 2017; Yasin et al., 2020). Since NDBI is responsive to built-up features (Macarof & Statescu, 2017), the minimum increase of this index over the years suggests further growth even in areas that are less developed. Generally, the more land that is converted to an urban area, the higher the NDBI value. This corresponds with the findings of other urban centers, such as Kathmandu Valley (Hamal et al., 2022) and Bangalore (Kanga et al., 2022). Figure 4 illustrates the spatial pattern of LST, NDVI, and NDBI for selected years (2013, 2016, 2019, and 2022). Figure 4 shows the spatial patterns of LST, NDVI, and NDBI for selected years (2013, 2016, 2019, and 2022).

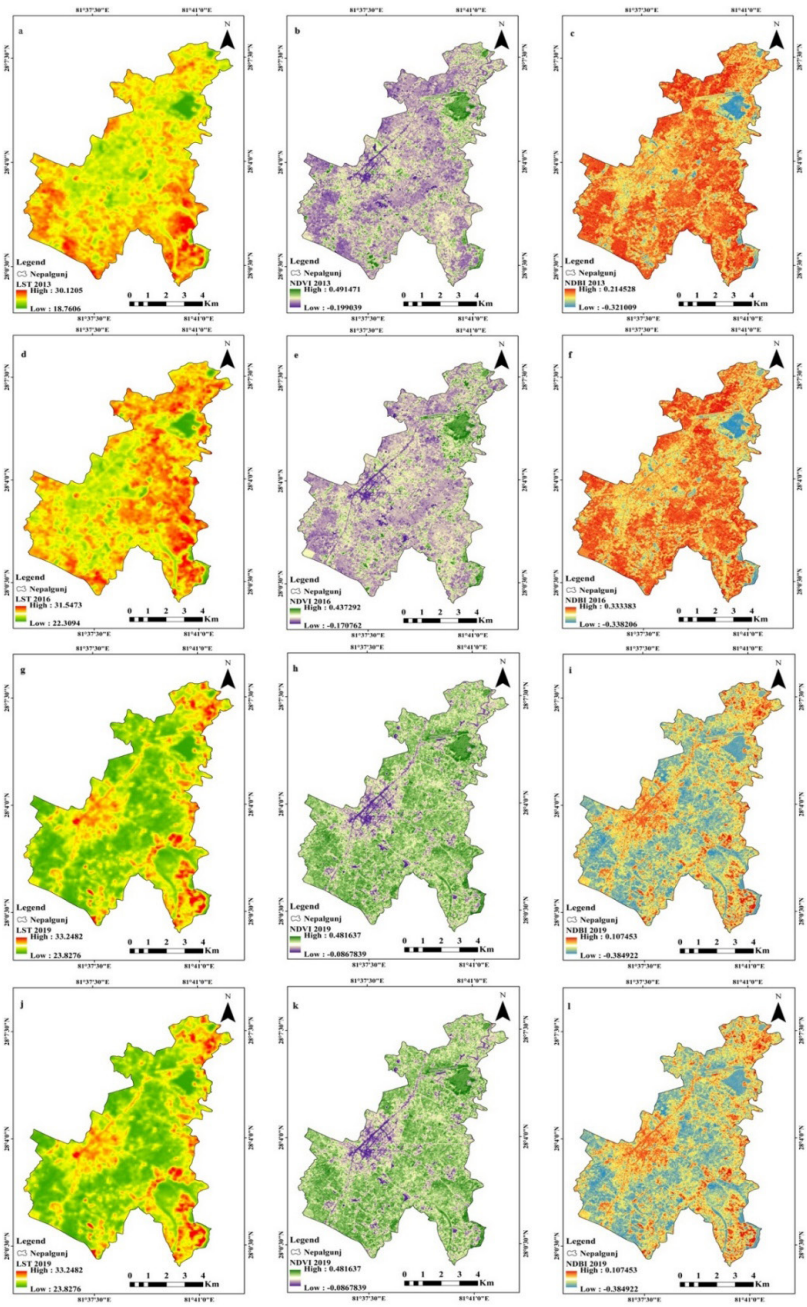

Figure 4. Map showing (a) LST (2013), (b) NDVI (2013), (c) NDBI (2013), (d) LST (2016), (e) NDVI (2016), (f) NDBI (2016), (g) LST (2019), (h) NDVI (2019), (i) NDBI (2019), (j) LST (2022), (k) NDVI (2022), (l) NDBI (2022)

Land surface temperature

The Figure 5 gives the LST's consistent upward trend in minimum and maximum values recorded during the years 2013 to 2022. The average LST increased by about 4.82 °C within nine years- from approximately 24.44 °C in 2013 to around 29.26 °C in 2022. Successive three-year intervals give a rise of at least 1 °C in the minimum and maximum LST values. The most rapid warming occurred from 2013 to 2016, followed by a slight slowing from 2019 to 2022, indicating that the rate of temperature rise has somewhat slowed down in recent years.

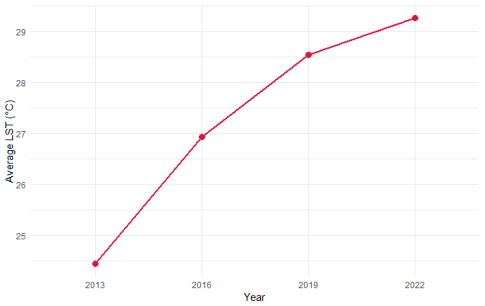

Figure 5. The change in land surface temperature (°C) from 2013 to 2022.

This pattern follows the typical trend of an urban heat island effect, which has been well-documented for cities experiencing rapid urbanization across the world (Aryal et al., 2021; Chand et al., 2021). During the growth of a city, green and water-surrounded areas are generally converted into heat-absorbing and heat-storing materials like asphalt and concrete (Wang & Akbari, 2017), which results in local temperatures continuing to rise and, in turn, strengthening the UHI effect. Here, the warming trend in Nepalgunj is very prominent, with an increase in warming by approximately 0.53 °C per year from 2013 to 2022. While this is less intense than the strong UHI reported in Kathmandu, it still points to a concerning warming indication related to city growth.

Correlation analysis

Correlation coefficients among LST, NDVI, and NDBI were gathered from the years 2013, 2016, 2019, and 2022 in order to study the relationship among them. Results are shown in Table 4 which quantifies both the magnitude and direction of associations between these variables quantifying both the strength and direction of the relationships.

Table 4. Correlation coefficients for LST, NDVI, and NDBI

Year	Correlation coefficients LST-NDVI	Correlation coefficients LST-NDBI	Correlation coefficients NDVI-NDBI
2013	-0.3528***	0.6042***	-0.8047***
2016	-0.3165***	0.6495***	-0.7431***
2019	-0.5524***	0.7743***	-0.8007***
2022	-0.4257***	0.6943***	-0.7601***

Scatter plots (Figure 6**)** further illustrate these statistical relationships. The patterns can be interpreted as follows:

LST and NDVI: For all study years, there is a moderate to strong negative relationship, with r^2 values ranging from -0.3165 to -0.5524 across (Figure 6-a, d, g, j). The consistent negative trend indicates that as temperature increases at the surface, vegetation health decreases, which further corroborates earlier studies (Carlson et al., 1994; Hu et al., 2023; Macarof & Statescu, 2017).

LST and NDBI: The relationship that exists between surface temperature and the built-up index is positive and statistically significant, with r^2 ranging from 0.6042 to 0.7743 (Figure 6-b, e, h, k). This means that increased LST corresponds to greater extents of urbanization as depicted by NDBI. This strong correlation supports that LST is a good indicator of the extension of built-up areas, which agrees with observations of similar studies (Kanga et al., 2022; Yasin et al., 2020).

NDVI and NDBI: Strong negative correlation ranges between -0.8047 to -0.7601. This indicates that with increasing built-up, there is a reduction in vegetation cover (Figure 6-c, f, i, l). Thus, NDVI still proves promising for land-use change monitoring, especially towards understanding the natural vegetation-urban growth balance. This is in line with recent studies done by Shah et al., 2022 and Bhomi, 2024.

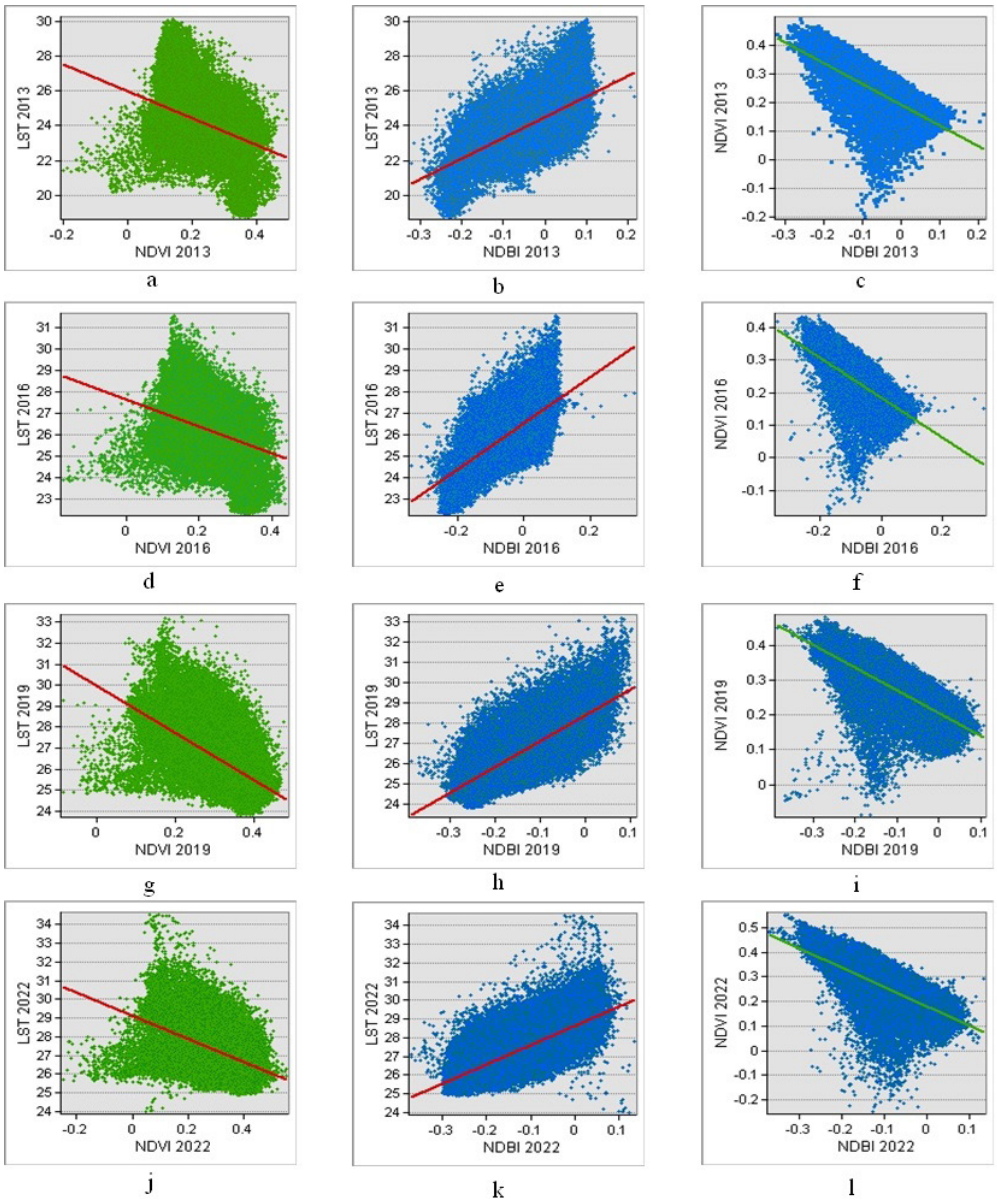

Figure 6. Scatter plots showing relationship between (a) LST and NDVI (2013), b) LST and NDBI (2013), (c) NDVI and NDBI (2013), (d) LST and NDVI (2016), (e) LST and NDBI (2016), (f) NDVI and NDBI (2016), (g) LST and NDVI (2019), (h) LST and NDBI (2019), (i) NDVI

Overall, these analyses indicate that the losses of vegetation are accompanying urban expansion, whereas increased hard surfaces tend to increase surface warming. This finding corresponds to the pattern established for several other parts of the world, such as Karanam & Neela, 2017 and Macarof & Statescu, 2017.

Conclusion

The strong positive relation of LST with NDBI established that the rise in urbanization directly contributes to surface warming and reflects the urgency of UHI conditions. The inverse relation of LST with NDVI is considered an effect of increasing temperatures on vegetation health. Similarly, a steady negative relation of NDVI with NDBI underlined the trade-off between the expanding area and decline of natural greenery in the city.

The findings indicate an immediate need for integrated, cohesive, and sustainable urban development strategies. Further sprawl without planning can cause increased temperatures, loss of biodiversity, and deterioration of environmental quality, ultimately affecting the health of the general public and stability of ecosystems. RS technologies in monitoring can enable data-driven policy decisions by policymakers to balance economic growth with ecological sustainability. These actionable insights contribute to the current understanding of the dynamics of the urban climate in South Asia and, therefore, will prove very useful for local authorities, planners, and researchers interested in the development of resilient and environmentally friendly urban systems.

References

Ahmadi, H., & Nusrath, A. (2010). Vegetation change detection of Neka River in Iran by using remote sensing and GIS. *Journal of Geography and Geology, 2*(1), 58–65.

Aryal, A., Shakya, B. M., Maharjan, M., Talchabhadel, R., & Thapa, B. R. (2021). *Evaluation of the land surface temperature using satellite images in Kathmandu Valley*. University of Yamanashi.

Bhattarai, K., & Conway, D. (2021). Contemporary environmental problems in Nepal. In *Contemporary environmental problems in Nepal* (pp. 201–334). Springer.

Bhandari, A. K., Kumar, A., & Singh, G. K. (2012). Feature extraction using normalized difference vegetation index (NDVI): A case study of Jabalpur City. *Procedia Technology, 6*, 612–621. https://doi.org/10.1016/j.protcy.2012.10.074

Bhomi, A. K., Poudyal, R., Tolange, S. K., & Chaudhary, S. (2024). Assessing the impact of urban expansion on forest cover using LULC maps, NDVI, and NDBI: A case study of Kathmandu District. *Journal on Geoinformatics, Nepal*, 1–7.

Cao, L., Li, P., Zhang, L., & Chen, T. (2008). Remote sensing image-based analysis of the relationship between

urban heat island and vegetation fraction. *International Archives of the Photogrammetry, Remote Sensing and Spatial Information Sciences, 37*, 1379–1384.

Carlson, T. N., Gillies, R. R., & Perry, E. M. (1994). A method to make use of thermal infrared temperature and NDVI measurements to infer surface soil water content and fractional vegetation cover. *Remote Sensing Reviews, 9*(1–2), 161–173. https://doi.org/10.1080/02757259409532220

Chand, M. B., Bhattarai, B. C., Pradhananga, N. S., & Baral, P. (2021). Trend analysis of temperature data for the Narayani River Basin, Nepal. *Sci, 3*(1), Article 1. https://doi.org/10.3390/sci3010001

Chapagain, D. (2018). Present situation of urbanization in Nepal. *International Journal of Humanities and Social Science Education, 5*, 170–175.

Chhetri, T. B., Dhital, Y. P., Tandong, Y., Devkota, L. P., & Dawadi, B. (2020). Observations of heavy rainfall and extreme flood events over Banke–Bardiya districts of Nepal in 2016–2017. *Progress in Disaster Science, 6*, Article 100074. https://doi.org/10.1016/j.pdisas.2020.100074

Department of Hydrology and Meteorology. (2014). *Average precipitation of Nepalgunj city*. DHM, Nepal.

Hamal, S., Chauhan, R., & Thakuri, S. (2022). Effect of urbanization on land surface temperature: A case study of Kathmandu Valley. *The Geographic Base*, 39–52.

Haylemariyam, M. B. (2018). Detection of land surface temperature in relation to land use land cover change: Dire Dawa City, Ethiopia. *Journal of Remote Sensing & GIS, 7*(3). https://doi.org/10.4172/2469-4134.1000245

Huete, A. R., & Liu, H. Q. (1994). An error and sensitivity analysis of the atmospheric- and soil-correcting variants of the NDVI for the MODIS-EOS. *IEEE Transactions on Geoscience and Remote Sensing, 32*(4), 897–905. https://doi.org/10.1109/36.298018

Hu, Y., Tang, R., Jiang, X., Li, Z. L., Jiang, Y., Liu, M., & Zhou, X. (2023). A physical method for downscaling land surface temperatures using surface energy balance theory. *Remote Sensing of Environment, 286*, Article 113421. https://doi.org/10.1016/j.rse.2022.113421

Hulley, M. E. (2012). The urban heat island effect: Causes and potential solutions. In *Metropolitan sustainability* (pp. 79–98). Woodhead Publishing.

Jat, M. K., Garg, P. K., & Khare, D. (2008). Monitoring and modelling of urban sprawl using remote sensing and GIS techniques. *International Journal of Applied Earth Observation and Geoinformation, 10*(1), 26–43. https://doi.org/10.1016/j.jag.2007.04.002

Jiménez-Muñoz, J. C., & Sobrino, J. A. (2009). A single-channel algorithm

for land surface temperature retrieval from ASTER data. *IEEE Geoscience and Remote Sensing Letters, 7*(1), 176–179. https://doi.org/10.1109/LGRS.2009.2029534

Kalma, J. D., McVicar, T. R., & McCabe, M. F. (2008). Estimating land surface evaporation: A review of methods using remotely sensed surface temperature data. *Surveys in Geophysics, 29*, 421–469. https://doi.org/10.1007/s10712-008-9037-z

Kandel, S., Gyawali, B., Sandifer, J., Shrestha, S., & Upadhaya, S. (2022). *Assessment of urban heat islands (UHIs) using satellite-derived NDVI and land surface temperature in three metropolitan cities of Nepal*.

Kanga, S., Meraj, G., Johnson, B. A., Singh, S. K., P. V., M. N., Farooq, M., & Sahu, N. (2022). Understanding the linkage between urban growth and land surface temperature: A case study of Bangalore City, India. *Remote Sensing, 14*(17), 4241. https://doi.org/10.3390/rs14174241

Karanam, H. K., & Neela, V. B. (2017). Study of normalized difference built-up index (NDBI) in automatically mapping urban areas from Landsat TM imagery. *International Journal of Engineering Sciences & Mathematics, 8*, 239–248.

Khan, R., Li, H., Basir, M., Chen, Y. L., Sajjad, M. M., Haq, I. U., & Hassan, W. (2022). Monitoring land use land cover changes and its impacts on land surface temperature over Mardan and Charsadda Districts, Pakistan. *Environmental Monitoring and Assessment, 194*(6), Article 409. https://doi.org/10.1007/s10661-022-10029-5

Kim, H. H. (1992). Urban heat island. *International Journal of Remote Sensing, 13*(12), 2319–2336. https://doi.org/10.1080/01431169208904271

Kuang, W., Liu, J., Dong, J., Chi, W., & Zhang, C. (2016). Rapid and massive urban and industrial land expansions in China between 1990 and 2010. *Landscape and Urban Planning, 145*, 21–33. https://doi.org/10.1016/j.landurbplan.2015.10.012

Leprieur, C., Kerr, Y. H., Mastorchio, S., & Meunier, J. C. (2000). Monitoring vegetation cover across semi-arid regions. *International Journal of Remote Sensing, 21*(2), 281–300.

Macarof, P., & Statescu, F. (2017). Comparison of NDBI and NDVI as indicators of surface urban heat island effect in Landsat 8 imagery. *Present Environment and Sustainable Development*, 141–150.

Nath, B. (2014). Quantitative assessment of forest cover change using NDVI techniques. *Journal of Geosciences and Geomatics, 2*(1), 21–27.

Putri, T. R., & Supriatna, S. (2021). A spatial study of rubber plant health using Sentinel-2A imagery. In *IOP Conference Series: Earth and Environmental Science* (Vol. 623, No. 1, Article 012078). IOP Publishing.

https://doi.org/10.1088/1755-1315/623/1/012078

Roy, P. S., Behera, M. D., & Srivastav, S. K. (2017). Satellite remote sensing: Sensors, applications and techniques. *Proceedings of the National Academy of Sciences, India, Section A: Physical Sciences, 87*, 465–472. https://doi.org/10.1007/s40010-017-0428-8

Sasky, P., Sobirin, S., & Wibowo, A. (2017). Pengaruh perubahan penggunaan tanah terhadap suhu permukaan daratan Metropolitan Bandung Raya tahun 2000–2016. In *Proceedings of the Industrial Research Workshop and National Seminar* (Vol. 8, pp. 354–361).

Shah, S. A., Kiran, M., Nazir, A., & Ashrafani, S. H. (2022). Exploring NDVI and NDBI relationship using Landsat 8 OLI/TIRS. *Malaysian Journal of Geosciences, 6*(1), 8–11.

Singha, S., Kanhaiya, S., Kumar, S., & Yadav, S. K. (2022). Spatial and temporal variation in NDVI and NDWI of the Ukhma River Basin, Central India. *Journal of Scientific Research, 66*(3).

Subedi, A., Khan, R., Hassan, A., & Hogesteeger, S. (2022). *Identification of heat threshold and heat hotspots in Nepalgunj, Nepal*.

Tariq, A., & Shu, H. (2020). CA-Markov chain analysis of seasonal land surface temperature and LULC change. *Remote Sensing, 12*(20), 3402. https://doi.org/10.3390/rs12203402

Valor, E., & Caselles, V. (1996). Mapping land surface emissivity from NDVI. *Remote Sensing of Environment, 57*(3), 167–184.

Wang, Y., & Akbari, H. (2017). Urban heat island mitigation in cold climates: A case of Montreal. *Advances in Environmental Research, 54*, 143–177.

Weather Atlas. (2023). *Nepalgunj, Nepal: Detailed climate information and monthly weather forecast*. https://www.weather-atlas.com/en/nepal/nepalgunj-climate

Wigginton, N. S., Fahrenkamp-Uppenbrink, J., Wible, B., & Malakoff, D. (2016). Cities are the future. *Science, 352*(6288), 904–905. https://doi.org/10.1126/science.352.6288.904

Yasin, M. Y., Abdullah, J., Noor, N. M., & Yusoff, M. M. (2020). Land cover and NDBI analysis to map built-up area. In *IOP Conference Series: Earth and Environmental Science* (Vol. 540, No. 1, Article 012073). IOP Publishing. https://doi.org/10.1088/1755-1315/540/1/012073

Zha, Y., Gao, J., & Ni, S. (2003). Use of normalized difference built-up index in automatically mapping urban areas. *International Journal of Remote Sensing, 24*(3), 583–594. https://doi.org/10.1080/01431160304987